IOSR Journal of Mechanical and Civil Engineering (IOSR-JMCE)
e-ISSN: 2278-1684,p-ISSN: 2320-334X, Volume 13, Issue 6 Ver. V (Nov. - Dec. 2016), PP 58-69
www.iosrjournals.org

Two Dimensional Numerical Modeling of a Micro Heat Pipe in Steady State Operation

Bamdad Barari[1]
[1]*Mechanical Engineering Department, University of Wisconsin Milwaukee, Milwaukee, WI*

***Abstract**: In this study, two dimensional numerical modeling has been used to investigate heat transfer and fluid flow in a micro heat pipe. Water and water vapor is considered as liquid and vapor phases in two phase flow investigation. For flow field analysis, the contours and diagrams for velocity, pressure and volume fraction of each phase has been presented. Heat transfer analysis is presented by temperature diagrams. In addition, effects of different geometries and various length scales have been considered by comparison of temperature diagrams. High oscillations and instabilities have been observed by the results of velocity and pressure. The instabilities are increased in evaporation and condensation region. High amount of phase change and combination of flow in micro heat pipe are some important reasons cause these oscillations. Finally, Effective heat transfer coefficient is calculated and has a well adoption with other numerical works.*
***Keywords:** Heat transfer, Micro fluidic, Micro heat pipe, Phase changes*

I. Introduction

Micro scale heat exchangers are commonly used in so many important technological processes which require greater heat transfer such as the electronic device, micro gravity environments, space craft thermal control and micro power generator [1, 2]. The micro-power generators show better performance than conventional batteries if only the efficiency is higher than 1%. The micro-power generator main part, namely micro-combustor, has many problems different from the conventional combustion chambers [3-5]. Micro heat pipe is closed channel with three parts, namely, evaporative, adiabatic and condenser section. Heat input vaporized coolant in evaporative section then vapor passes through the adiabatic to the condenser section caused by changing in pressure. In the condenser section, the vapor condensed and gets liquid. The liquid flows towards the evaporative section, due to capillary effects between liquid molecules and substrates of channel. The net capillary force is generated by the combined effect of the evaporating and the condensing menisci [6]. Practically, a micro heat pipe is a non-circular channel with a diameter of 10–500 μm and length of 10 to 20 mm. Cotter first considered the concept of micro heat pipe, which is used as heat exchanger for the uniform temperature distribution in electronic chips [7]. Micro heat pipes, which could be set in silicon substrate, have been investigated by Mallik and Peterson [8], [9] and Peterson et al. [10] in several studies. They have also used experimental verification on a micro heat pipes with a cross-sectional dimension of about one millimeter charging with water as coolant. Babin et al. [11] have studied on a steady-state micro heat pipe to evaluate heat transport capacity. Longtin et al. [12] have developed one-dimensional steady state model, which calculated working fluid velocity, pressure and film thickness along the length of the micro heat pipe. Wu et al. [13] have investigated on the maximum heat transfer and the minimum meniscus radius in triangular grooves. They also used the Young–Laplace equation to analyze the fluid dynamics of such devices inside the channel [14]. Khrustalev and Faghri [15]studied on thermal analysis and limitations of a micro heat pipe. Xu and Carey [16] have analyzed evaporation of thin film region of the meniscus for a V-shaped micro groove surface based on analytical model. Stephan and Busse [17] calculated the radial heat transfer coefficient in heat pipes with open grooves. They have revealed that the assumption of an interface temperature equal to the saturation temperature of the vapor leads to a large over-prediction of the radial heat transfer coefficient. Ravikumar and DasGupta [18] presented the model to investigate V-shaped micro grooves [19, 20]. The model includes the evaporation from the capillary and the transition region of the extended meniscus as a function of groove length. In recent years, many researchers like Ma and Peterson [14] have investigated the concept of using micro heat pipes as effective heat spreaders. Ha and Peterson [21] presented an analytical solution on a quadratic profile of the evaporative heat flux for small tilt angles. Their studies showed design restrictions and utility of micro heat pipes. Catton and Stroes [22] used one-dimensional, semi analytical model for prediction of the wetted length supported by inclined triangular capillary grooves. Suman et al. [23] has studied on a generalized model of a micro heat pipe of polygonal shape. They have performed detailed study of triangular and rectangular heat pipes [24]. Technical investigations related to micro heat pipes, include liquid distribution and charge optimization [25, 26], interfacial thermodynamics in micro heat pipe capillary structures [26] and micro heat pipe transient behavior [27]. Machado studied on flat micro heat pipe using time dependent numerical modeling in which the interface of two phases is indicated by interface tracking method [28]. Gebresilassie presented finite element

method to investigate on heat transfers and flow field micro heat pipe [29]. Study of the flow and heat transfer is very important in different devices [30, 31]. There are some recent numerical and experimental studies [32-35] on heat transfer on homogeneous charge compression ignition (HCCI) engines in which the heat release rate and pressure traces for a biofuel are investigated [36-40]. Experimental investigations of heat transfer behavior in channels flows have been of interest [41]. CFD studies however cover a wide range of different industries, such as sports [42], combustion, and engine studies. In present study two dimensional numerical modeling has been used for analyzing the flow field and heat transfer in micro heat pipe. Temperature, velocity, phase and pressure contours and diagrams have been presented in two-dimensional micro heat pipe. Also temperature and velocity distribution for vapor and liquid phase has been obtained.

II. Theory

A flat micro heat pipe heat sink consisting of an array of micro heat pipe channels used as a compact heat dissipation device that can effectively remove heat from an electronic chip. Each channel in the array performed as an independent heat transport device. The micro heat pipe consists of a heated evaporator section, adiabatic and a condenser section. The hot and the cold end denote the farthest end of evaporative and the condenser region, respectively. Due to capillary pumping, the liquid will be pushed towards the hot end. The liquid will travel along the corners and the vapor passes through the open space. Dimensions and boundary condition for each part of micro heat pipe have been shown in Fig. 1 and Table 1, respectively.

Table1. Boundary condition

Boundary	*Type of boundary*	*Thermal boundary condition*
AG	Wall	**Constant heat flux**
DI	Wall	**Constant heat flux**
GH	Wall	**Q=0**
IJ	Wall	**Q=0**
AD	Wall	**Q=0**
BC	Wall	**Q=0**
HB	Wall	**Convection**
JC	Wall	**Convection**
GI	Interface	**Coupled**
HJ	Interface	**Coupled**

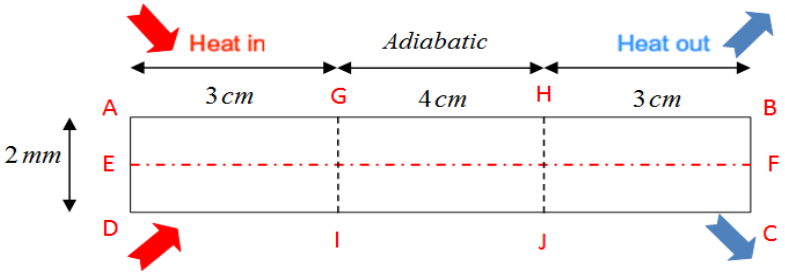

Figure 1- Geometry, dimensions, and boundary conditions of 2D micro heat pipe

The flow and heat transfer processes are governed by the continuity, momentum and energy equations for the liquid and vapor phases. As phase change occurs, the local mass rates of the individual liquid and vapor phases are coupled through a mass balance at the liquid-vapor interface. The cross-sectional areas of the vapor and liquid regions and the interfacial area vary along the axial length, due to the progressive phase change occurring as the fluid flows along the channel. In this study continuity equation, momentum equation and the energy equation have been investigated for analyzing the flow field and heat transfer in micro heat pipe.
The continuity equation for mixture in micro heat pipe is presented by (1):

$$\frac{\partial}{\partial t}(\rho_m)+\nabla\cdot\left(\rho_m \vec{v}_m\right)=0 \qquad (1)$$

Where $\vec{v}_m$ is the mass- averaged velocity which presented by (2):

$$\vec{v}_m=\frac{\sum_{k=1}^{n}\alpha_k\rho_k\vec{v}_k}{\rho_m} \qquad (2)$$

Where α_k and ρ_k is volume fraction and density of phase k, respectively. ρ_m could be obtain by (3):

$$\rho_m = \sum_{k=1}^{n} \alpha_k \rho_k \tag{3}$$

The momentum equation for the mixture can be obtained by summing the individual momentum equations for all phases. It can be expressed as

$$\frac{\partial}{\partial t}\left(\rho_m \vec{v}_m\right) + \nabla \cdot \left(\rho_m \vec{v}_m \vec{v}_m\right) = -\nabla p + \nabla \cdot \left[\mu_m (\nabla \vec{v}_m + \nabla \vec{v}_m^{\,T})\right] + \rho_m \vec{g} + \vec{F} + \nabla \cdot \left(\sum_{k=1}^{n} \alpha_k \rho_k \vec{v}_{dr,k} \vec{v}_{dr,k}\right) \tag{4}$$

Where *n* is the number of phases, $\vec{F}$ is a body force, and μ_m is the viscosity of the mixture:

$$\mu_m = \sum_{k=1}^{n} \alpha_k \mu_k \tag{5}$$

$\vec{v}_{dr,k}$ is the drift velocity for secondary phase *k* which obtained by (6):

$$\vec{v}_{dr,k} = \vec{v}_k - \vec{v}_m \tag{6}$$

The energy equation for the mixture takes the following form:

$$\frac{\partial}{\partial t}\sum_{k=1}^{n}\left(\alpha_k \rho_k E_k\right) + \nabla \cdot \sum_{k=1}^{n}\left(\alpha_k \vec{v}_k \left(\rho_k E_k + p\right)\right) = \nabla \cdot \left(k_{eff} \nabla T\right) + S_E \tag{7}$$

The first term on the right-hand side of (7) represents energy transfer due to conduction. S_E includes any other volumetric heat sources. In (7), E_k could be presented as (8) for compressible phase

$$E_k = h_k - \frac{p}{\rho_k} + \frac{v_k^{\,2}}{2} \tag{8}$$

And, for incompressible phase

$$E_k = h_k \tag{9}$$

Where h_k is the sensible enthalpy for phase *k*.

k_{eff} is effective thermal conductivity which presented by (10):

$$k_{eff} = \frac{Q_{in}}{A_c\left[\frac{T_e - T_c}{L}\right]} \tag{10}$$

Where Q_{in} is heat input to evaporator, A_c is cross section area of micro heat pipe, L is length and T_e-T_c is the temperature difference between evaporator and condenser section.

From the continuity equation for secondary phase *p*, the volume fraction equation for secondary phase p can be obtained as (11):

$$\frac{\partial}{\partial t}\left(\alpha_p \rho_p\right) + \nabla \cdot \left(\alpha_p \rho_p \vec{v}_m\right) = -\nabla \cdot \left(\alpha_p \rho_p \vec{v}_{dr,p}\right) + \sum_{q=1}^{n}\left(\dot{m}_{qp} - \dot{m}_{pq}\right) \tag{11}$$

Where $\dot{m}_{qp}$ is the mass transfer from phase *q* to phase *p* and $\dot{m}_{pq}$ is the mass transfer from phase *p* to phase *q*.

III. Numerical Modeling

The analysis presented here considered an individual channel and studied on heat transfer and fluid flow. The individual micro heat pipe channel analyzed in the present work has a characteristic length of 10 mm. The channel is fabricated on a silicon substrate and the working fluid is ultrapure water. A two-dimensional model is used for the analysis due to the geometry of the channels. The two dimensional analysis for fluid flow helped to understand phase change phenomenon at the micro scale within the micro heat pipe. Velocity, volume fraction and pressure contours are showed at ABCD section. Computation is performed for heat input equal to 1.5 W in the evaporator and it is supposed that vapor converted to water in condenser by releasing its latent heat. The values of heat transfer coefficients in the condenser is set to 20 W/m2-K obtained through forced air convection with an average temperature of 20 C and the specific latent heat of vaporization set to 2430500 J/kg.

Condensed vapor at the end of the channel returned to evaporation section by capillary force. In present two dimensional model, capillary effects is simulated by source terms of surface tension. In addition, for initialization of the numerical solving, it is assumed that liquid phase is located under the EF line in Fig. 1 where the vapor phase is accumulated the upper side of the EF line.

The computational process proceeded in steady state, as indicated by constant temperature value throughout. It was assumed that the thermo-physical properties of the working fluid both in the liquid and vapor phases did not vary significantly with temperature, within the operating range investigated. However, the variation of vapor density with temperature was incorporated in the computational scheme by interpolating from available thermo-physical property data. Based on the control volume method, the SIMPLE algorithm is employed to deal with the problem of velocity and pressure coupling. A first order upwind scheme and un-structured triangular uniform grid system are used to discretize the main governing equations. In order to obtain satisfactory solutions, a grid independence study is conducted in the analysis by adopting different grid distributions of the whole geometry. The numerical computation is ended if the residual summed over all the computational nodes satisfies the criterion less than 10^{-5}.

IV. Results and Discussions

In the present study, proper operation of the micro heat pipe has been shown by contours of volume fraction for each phase. In addition, the contours and diagrams of velocity, pressure and temperature have been presented. Finally, the effects of various length scales on temperature and pressure distribution have been obtained along the micro heat pipe.

4.1. Micro heat pipe volume fraction

The validity of applied numerical model was first investigated by using volume fraction of each phase in each part of entire micro heat pipe. Based on the literature liquid phase is accumulate the parts near the wall and also at the end of the micro heat pipe in condenser section as well as the vapor phase is passed through the middle parts of the entire channel. Since, filling ratio of the micro heat pipe is set to 40% and heat input equal to 1.5 W, Fig. 2 and 3 present volume fraction of each phase in evaporator section and condenser section. From the contour presented in Fig. 2, warm colors illustrated vapor phase and cold colors presented liquid phase. Up and bottom side of the contour illustrates higher amount of liquid instead of vapor, as expected. Volume fraction amount at the top and bottom equals to unity which guarantee proper performance for micro heat pipe. Micro heat pipe stop working when liquid volume fraction in evaporation section equal to zero. Vapor phase is passed through the middle side of the channel. It was expected that the amount of vapor in evaporator section is higher than water which the contour of volume fraction for evaporation section correctly predicted that. The contour of Fig. 3 shown that the amount of liquid phase increased and vapor decreased at the end of the channel. Cold color indicates liquid phase and warm color indicates vapor in the condenser section of micro heat pipe. The phase changes between liquid and vapor are observed at the end of the channel by some colors between red and blue in spectrum bar. In this position vapor condensed on the substrate and liquid pumped to evaporator by capillary effects. Because of opposite direction of liquid and vapor the interfaces are more complicated at the end of the channel.

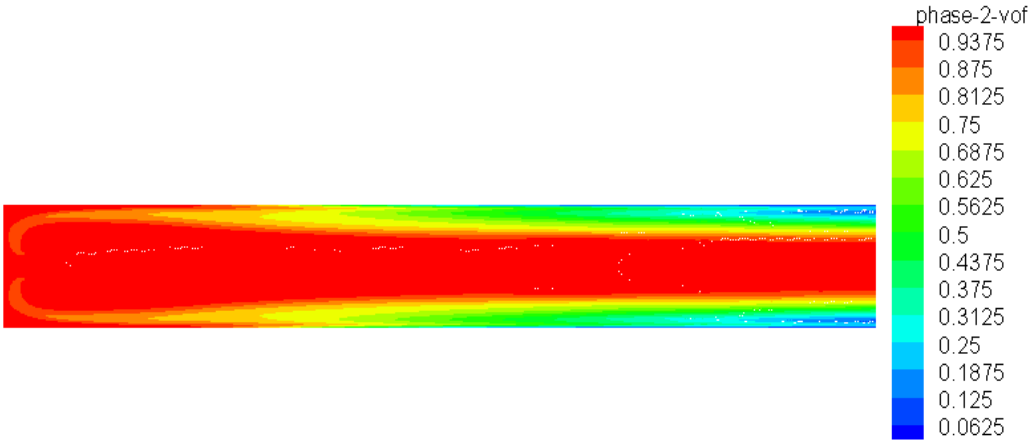

Figure 2- Water- vapor volume fraction in evaporator section

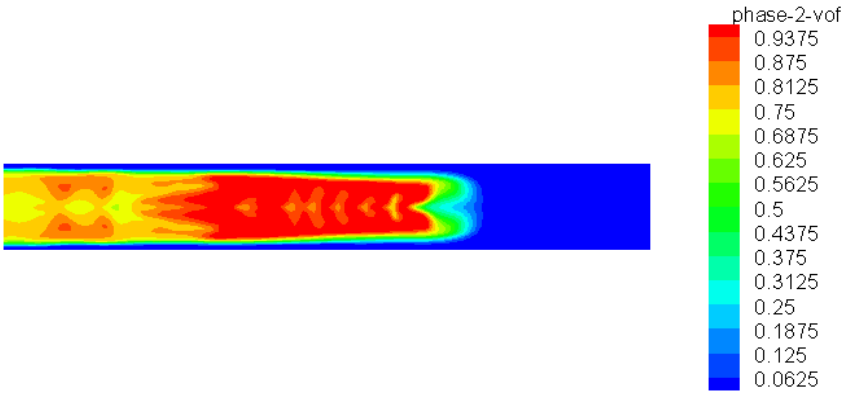

Figure 3- Water- vapor volume fraction in condenser section

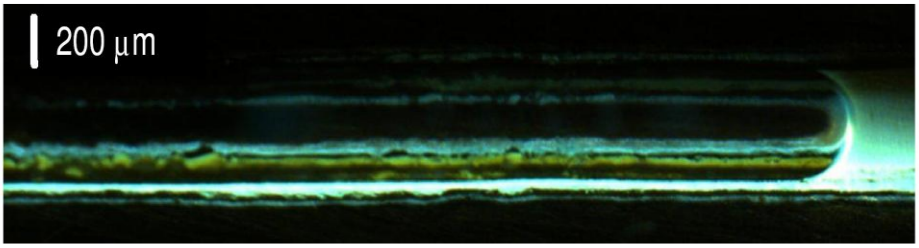

Figure 4- Experimental capturing of two phase in micro heat pipe [43]

Fig. 4 illustrates experimental capturing of two phases in micro heat pipe. Water phase could be observed on up and downside and also at the end of the channel as mentioned in contours of figures 2 and 3. Contours have an appropriate adoption with experimental results. The behavior of liquid phase in entire micro heat pipe is shown in figure 5. As mention before, liquid phase, which mentioned by warm color in this contour, concentrated in the up and bottom side and vapor (cold color) situated in the middle of the ABCD section. The amount of volume fraction for whole channel showed the position of each phase in channel. Also, the interface of the phases and mass transfer rate which indicate the rate of phase change could be observed in the contour. The latent heat is directly related to the amount of heat transfer capacity. However, the beginning of the condenser and evaporator sections corresponded to high values of phase change rate. The liquid entered the evaporator in the sharp corners followed by an important rate of vaporization from heat input at the beginning of the evaporator section. The evaporation process started at the corners and continued towards the middle of the micro heat pipe. The condensation process took place at the beginning of the condenser. The perturbation could be observed at the end of the condenser section which expressed high amount of phase changes occurred in this position. Fig.6 presented contour of volume fraction in adiabatic section. In the adiabatic section, the rate of phase change phenomenon was negligible and uniform passes of liquid and vapor phase could be seen in contours.

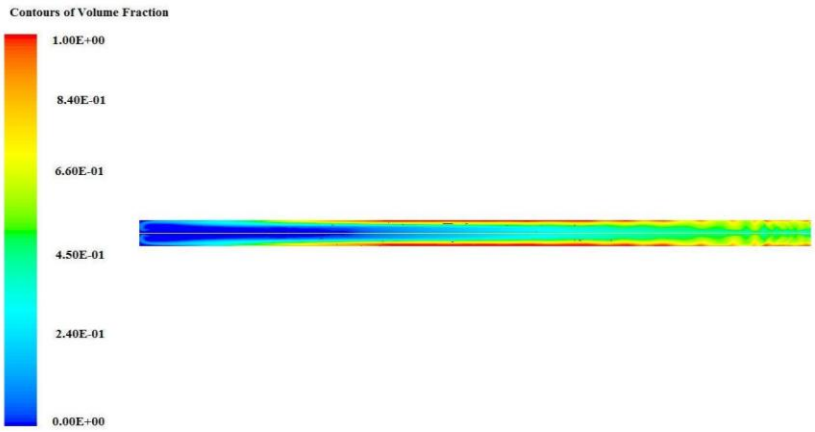

Figure 5- Volume fraction of liquid phase for entire channel

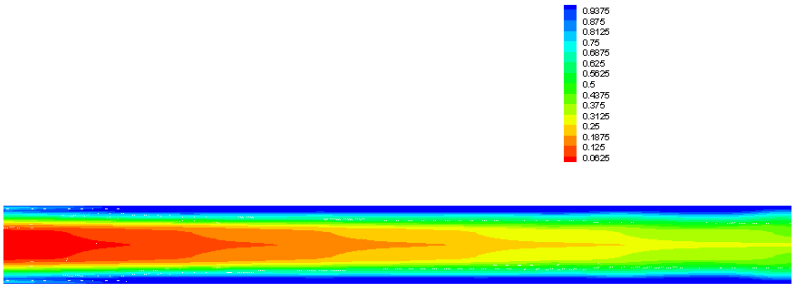

Figure 6- Water- vapor volume fraction in adiabatic section

4.2. Micro heat pipe velocity distribution

Results for axial velocity of vapor phase in evaporation and condensation part of micro heat pipe have been shown in Fig. 7 and 8. As the results for ABCD cross section shown, the velocity is high at the middle part of the section and decreased near the wall and equal to zero at the substrate. Some swirling flow can be mentioned in frontier parts of evaporator section. The liquid which came from condenser evaporates in this part and passes through the middle part of channel to condenser. The velocity of vapor decreased when vapor entered to condenser section and then began to condense in condenser. Contour of axial velocity in condenser section showed exactly what happen to vapor in condenser. According to the velocity contours for each part, it could be understood that phases traveled in opposite path along the micro heat pipe. While the liquid phase runs from the condenser to the evaporator, the vapor passes through the middle of the channel and returns from the evaporator to the condenser. The contour shown in Figures 7 and 8 clearly demonstrates the similar behavior. The cold colors illustrate velocity of liquid passes from condenser towards the evaporator and prove that in up and down of channel the fluid is moving towards the evaporator. However, the warm colors indicate vapor velocity which passes from the evaporator to the condenser at the middle of the channel and show that the flow in the middle of the channel passed towards the condenser. This phenomenon helped the circulation processed until all of the liquid water in evaporation section disappeared. In this situation, dry-out phenomenon took place and micro heat pipe operation is terminated.

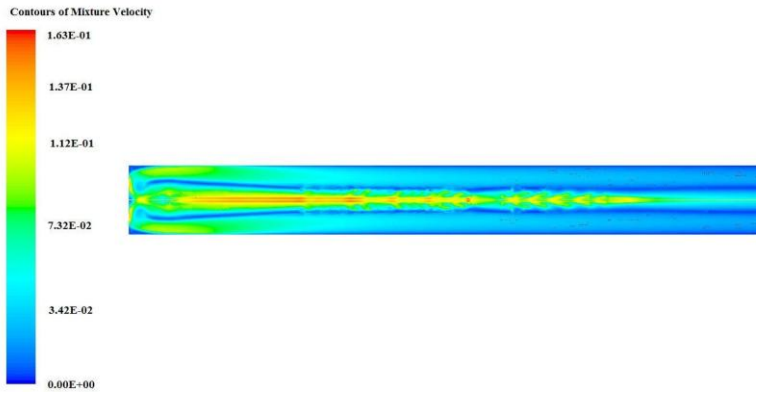

Figure 7- Velocity distribution of phases in evaporator section

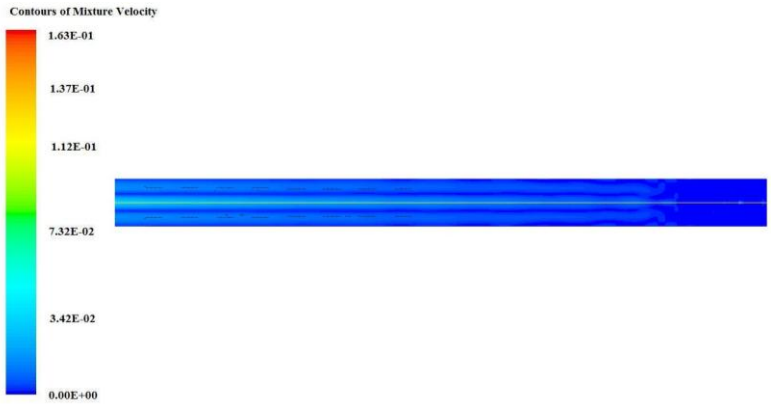

Figure 8- Velocity distribution of phases in condenser section

Further investigation for velocity distribution in micro heat pipe is presented in Fig 9. Some oscillation could be observed in velocity distribution diagram. In the evaporator, the vaporized liquid moves from up and down towards the central regions of the channel and lead to a complicated flow pattern in the central regions of the channel which caused high oscillation in mixture velocity in evaporation part. As can be seen, the oscillation vanished in adiabatic and condenser section and the velocity equal to zero at the end of the channel. This phenomenon could be explained by Fig. 10. Stresses between two phases and continues phase changes in evaporator and condenser are the most significant reason for unsteadiness and oscillations of velocity result. These parameters could be observed in schematic micro heat pipe presented in Fig 10.

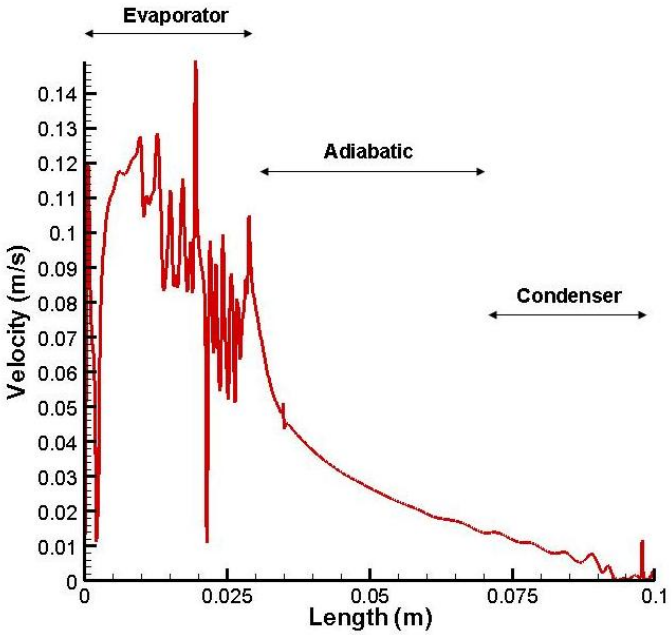

Figure 9- Vapor velocity along EF line in ABCD section

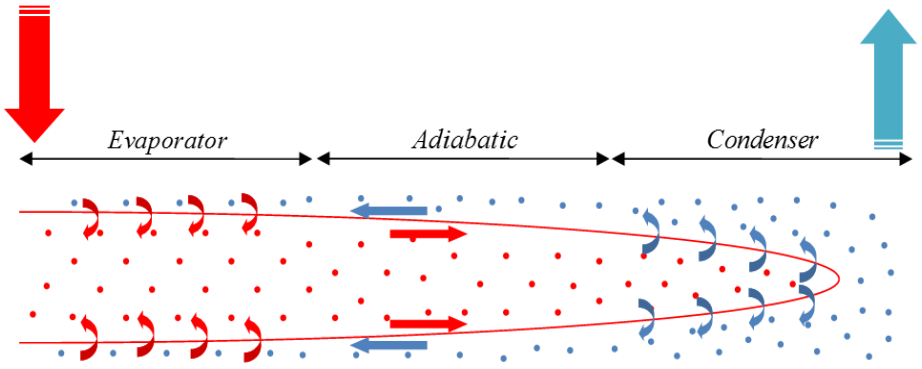

Figure 10- Schematic view of micro heat pipe

4.3. Micro heat pipe pressure distribution

In this part the results of the pressure field in the ABCD plate are presented in Fig.11 for entire channel. The plus and minus amount of pressure in contour illustrated the pass line of vapor and liquid phase, respectively. Three main colors along the axial direction of the micro heat pipe show that the pressure gradient in each section of the micro heat pipe is small, while there is a pressure difference between different sections. In addition, it could be understood that, vapor pass through the condenser while water bypass to evaporator section. The pressure distribution for the mixture through the EF line has been presented in Fig.12. Mixture pressure changed from 2.5 Pa at x = 0 to -0.5 Pa at x = 10 mm. The reduction of pressure from the evaporator to the condenser indicated the direction of vapor flow in the channel. The steady state pressure difference between evaporator and condenser guaranteed a continuous flow of the vapor. A small pressure drop in the adiabatic section was caused by pressure losses within the channel. The results for another length scale of L/D=100 and L/D= 25 are presented by Fig. 13 and 14.

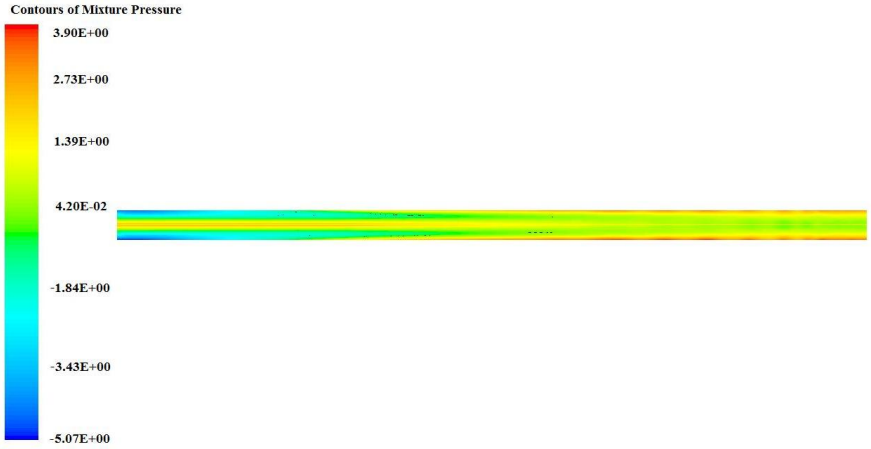

Figure 11- Pressure distribution for entire channel

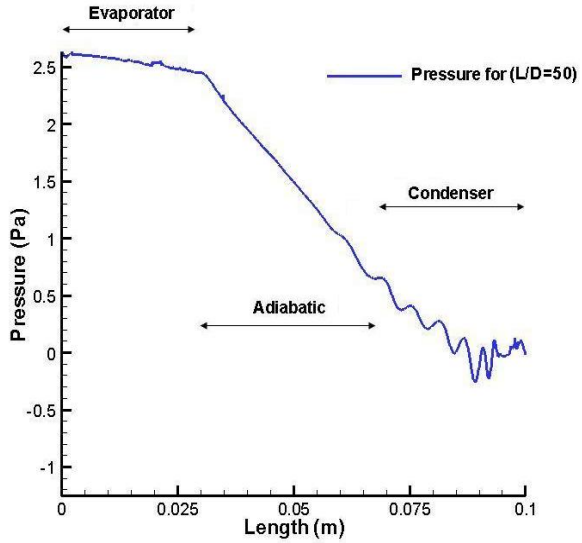

Figure 12- Pressure distribution along EF line for L/D=50

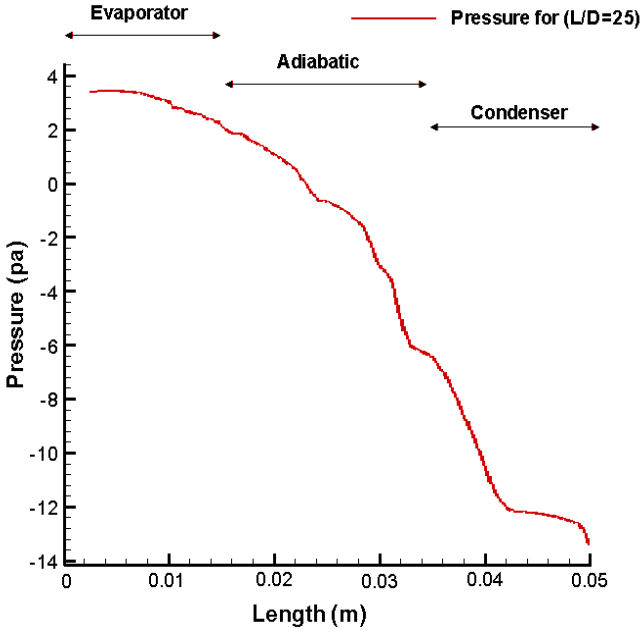

Figure 13- Pressure distribution along EF line for L/D=25

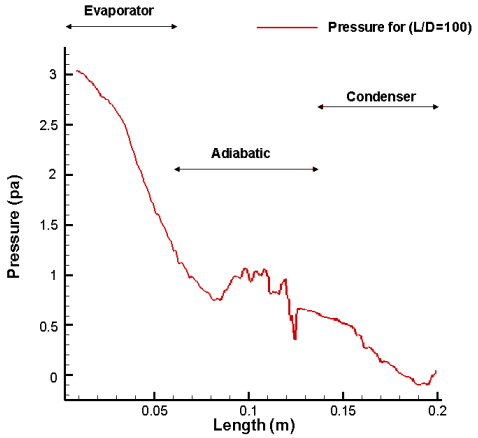

Figure 14- Pressure distribution along EF line for L/D=100

4.4. Micro heat pipe temperature distribution

Temperature distribution result for length scale equal to 50 has been presented in Fig. 15. The mixture temperature varied from 355 k to 320 k at downside of the micro heat pipe. Results for length scale set to 25 and 100 were presented in Fig. 16 and 17. It could be observed that the temperature in evaporator section increased by increasing length of micro heat pipe. In this situation, dry-out phenomenon will be occurred and the hot spot in evaporator section rose up the temperature. Additional analysis on dry-out phenomenon has been made by investigation on volume fraction contour for this case. Volume fraction contour for length scale equal to 100 has been shown in Fig. 18. It is so noticeable that, water phase couldn't cover the entire substrate of evaporator section and hot spot caused increasing in temperature.

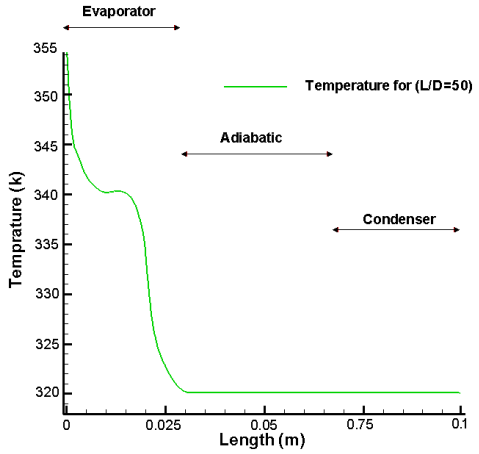

Figure 15- Temperature distribution along EF line for L/D=50

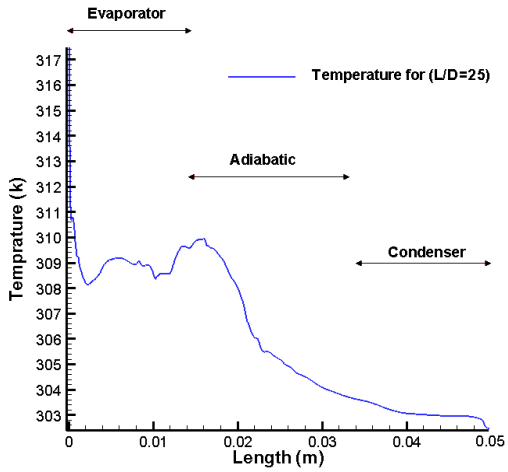

Fig.16. Temperature distribution along EF line for L/D=25

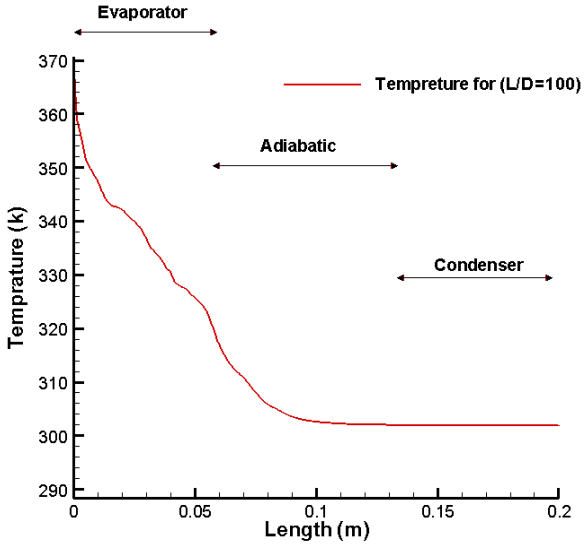

Figure 16- Temperature distribution along EF line for L/D=100

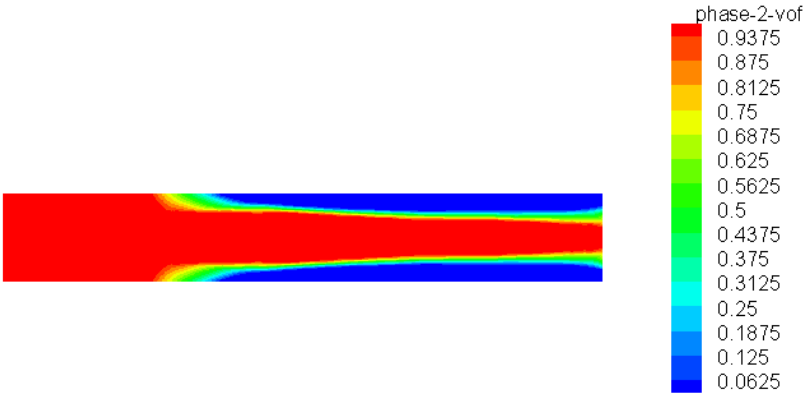

Figure 17- Volume fraction of phases for L/D=100

Effective thermal conductivity is an appropriate index to study on proper operation of micro heat pipe. Based on (10), effective thermal conductivity has been obtained 3088 W/m-k for length scale equal to 50 and heat input set to 1.5 W which is eight times higher than copper. It is obvious that with increasing heat flux in the evaporator, liquid water in the evaporator is replaced with the vapor with higher temperature and the effective thermal conductivity of the micro heat pipe decreases. Based on the micro heat pipe dimension [43] and the mixture theory, an effective thermal conductivity of 3158 W/m-k was calculated for micro channels investigated by Duncan and Peterson [25] and [10] The difference between the effective thermal conductivities obtained from this model and the previous studies was 4%, which indicates the validity of the model to quantitatively investigate the thermal performance of micro heat pipes.

V. Conclusion

The single micro heat pipe was investigated by using of two- dimensional numerical model. For the single micro heat pipe, the phenomenon of liquid accumulation in the corners and the phase change process within the micro heat pipe were accurately captured. Based on numerical model, the velocity field, vapor pressure gradient and temperature distribution were obtained for various length scales. Capturing two-phase flow in the interconnected geometry helped to understand the phase separation in the micro heat pipe. Two-phase circulation of the working fluid illustrated the proper operation of the micro heat pipe. Results of this work demonstrated the abilities of two dimensional approach to simulate two-phase flow and heat transfer of micro heat pipes. By improving the assumptions such as properties of liquid and vapor, boundary conditions by considering heat flux through the side walls of the micro heat pipe and the input parameters like temperature dependent properties definitely leads to more realistic simulations. Finally, it can be concluded that two dimensional approach is so useful for observing the interaction of phases in flow field and defined the performance of micro heat pipe correctly.

References

[1]. Kamali, R., Barari, B., and Shirazi, A. A., "Numerical Analysis of Entropy Generation in Array of Pin-Fin Heat Sinks for Some Different Geometries," Proc. ASME 2010 3rd Joint US-European Fluids Engineering Summer Meeting collocated with 8th International Conference on Nanochannels, Microchannels, and Minichannels, American Society of Mechanical Engineers, pp. 1623-1628.

[2]. Rahimzadeh, H., Barari, B., and Asoodeh, M. H., "Numerical Analysis of Two-Phase Turbulent Flow in Horizontal Channel with Experimental Verification," Proc. Proceedings of the World Congress on Engineering.

[3]. Bidabadi, M., Barari, G., Azimi, M., and Mafi, M., 2009, "Theoretical Study of a Perfectly Volatile Particle Triple Flame," International Journal of Recent Trends in Engineering, 1(5), pp. 26-29.

[4]. BIDABADI, M., BARARI, G., and RAHBARI, A., "Analytical study of the triple flame for micro-droplet fuel stream considering heat loss," Proc. Experimental fluid mechanics.

[5]. Rahbari, A., and Barari, G., "Theoretical Study of Triple-Flame Temperature Distribution in Heat-Recirculated Microcombustor," Journal of Energy Engineering, 0(0), p. 04016009.

[6]. Swanson, L., and Herdt, G., 1992, "Model of the evaporating meniscus in a capillary tube," Journal of heat transfer, 114(2), pp. 434-441.

[7]. Cotter, T., 1984, "Principles and prospects for micro heat pipes," NASA STI/Recon Technical Report N, 84, p. 29149.

[8]. Peterson, G., and Mallik, A., 1995, "Transient response characteristics of vapor deposited micro heat pipe arrays," Journal of Electronic Packaging, 117(1), pp. 82-87.

[9]. Mallik, A., Peterson, G., and Weichold, M., 1992, "On the use of micro heat pipes as an integral part of semiconductor devices," Journal of Electronic Packaging, 114(4), pp. 436-442.

[10]. Peterson, G., Duncan, A., and Weichold, M., 1993, "Experimental investigation of micro heat pipes fabricated in silicon wafers," Journal of Heat Transfer, 115(3), pp. 751-756.

[11]. Babin, B., Peterson, G., and Wu, D., 1990, "Steady-state modeling and testing of a micro heat pipe," Journal of Heat Transfer, 112(3), pp. 595-601.

[12]. Longtin, J., Badran, B., and Gerner, F., 1994, "A one-dimensional model of a micro heat pipe during steady-state operation," Journal of Heat Transfer, 116(3), pp. 709-715.

[13]. Wu, D., and Peterson, G., 1991, "Investigation of the transient characteristics of a micro heat pipe," Journal of Thermophysics and Heat Transfer, 5(2), pp. 129-134.

[14]. Peterson, G., and Ma, H., 1996, "Theoretical analysis of the maximum heat transport in triangular grooves: a study of idealized micro heat pipes," Journal of heat transfer, 118(3), pp. 731-739.

[15]. Khrustalev, D., and Faghri, A., 1994, "Thermal analysis of a micro heat pipe," Journal of Heat transfer, 116(1), pp. 189-198.

[16]. Xu, X., and Carey, V., 1990, "Film evaporation from a micro-grooved surface-An approximate heat transfer model and its comparison with experimental data," Journal of Thermophysics and Heat Transfer, 4(4), pp. 512-520.

[17]. Stephan, P., and Busse, C., 1992, "Analysis of the heat transfer coefficient of grooved heat pipe evaporator walls," International Journal of heat and mass transfer, 35(2), pp. 383-391.

[18]. KUMAR, M. R., and DASGUPTA, S., 1997, "Modeling of evaporation from V-shaped microgrooves," Chemical Engineering Communications, 160(1), pp. 225-248.

[19]. Barari, B., Ellingham, T. K., Ghamhia, I. I., Pillai, K. M., El-Hajjar, R., Turng, L.-S., and Sabo, R., 2016, "Mechanical characterization of scalable cellulose nano-fiber based composites made using liquid composite molding process," Composites Part B: Engineering, 84, pp. 277-284.

[20]. Barari, B., and Pillai, K. M., 2015, "Search for a 'Green'Composite Material: An Attempt to Fabricate Cellulose Nano-Fiber Composites using Liquid Composite Molding," Journal of the Indian Institute of Science, 95(3), pp. 313–320.

[21]. Ha, J., and Peterson, G., 1998, "Analytical prediction of axial dry-out point for evaporating liquids in axial microgrooves," J. Heat Transfer, 120, pp. 452-457.

[22]. Catton, I., and Stroes, G. R., 2002, "A semi-analytical model to predict the capillary limit of heated inclined triangular capillary grooves," Journal of heat transfer, 124(1), pp. 162-168.

[23]. Suman, B., De, S., and DasGupta, S., 2005, "A model of the capillary limit of a micro heat pipe and prediction of the dry-out length," International Journal of Heat and Fluid Flow, 26(3), pp. 495-505.

[24]. Suman, B., De, S., and DasGupta, S., 2005, "Transient modeling of micro-grooved heat pipe," International journal of heat and mass transfer, 48(8), pp. 1633-1646.

[25]. Duncan, A., and Peterson, G., 1995, "Charge optimization for a triangular-shaped etched micro heat pipe," Journal of thermophysics and heat transfer, 9(2), pp. 365-368.

[26]. Swanson, L., and Peterson, G., 1993, "The interfacial thermodynamics of the capillary structures in micro heat pipes," ASME-PUBLICATIONS-HTD, 253, pp. 45-45.

[27]. Wu, D., Peterson, G., and Chang, W., 1991, "Transient experimental investigation of micro heat pipes," Journal of thermophysics and heat transfer, 5(4), pp. 539-544.

[28]. Machado, H. A., "Simulation of a Flat Capillary Heat Pipe Using an Interface Tracking Method," Proc. Proceedings of the XVII COBEM-Brazilian Congress of Mechanical Engineering, São Paulo, Brazil.

[29]. Markos-Gebresilassie, M., 2007, "Steady liquid flow and liquid-vapor interface shapes in different groove structures in micro heat pipes," SOUTHERN METHODIST UNIVERSITY.

[30]. Almansour, B., Thompson, L., Lopez, J., Barari, G., and Vasu, S. S., "Ignition and Flame Propagation in Oxy-Methane Mixtures Diluted With CO2," Proc. ASME Turbo Expo 2015: Turbine Technical Conference and Exposition, American Society of Mechanical Engineers, pp. V04BT04A021-V004BT004A021.

[31]. Almansour, B., Thompson, L., Lopez, J., Barari, G., and Vasu, S. S., 2016, "Laser Ignition and Flame Speed Measurements in Oxy-Methane Mixtures Diluted With CO2," Journal of Energy Resources Technology, 138(3), p. 032201.

[32]. Keshavarz, A., Mehrabian, M., Abolghasemi, M., and Mostafavi, A., 2011, "Availability (exergy) analysis in a thermal energy storage system with the phase change materials arranged in series," Proceedings of the Institution of Mechanical Engineers, Part A: Journal of Power and Energy, 225(1), pp. 44-52.

[33]. Abolghasemi, M., Keshavarz, A., and Mehrabian, M. A., 2012, "Thermodynamic analysis of a thermal storage unit under the influence of nano-particles added to the phase change material and/or the working fluid," Heat and Mass Transfer, 48(11), pp. 1961-1970.

[34]. Abolghasemi, M., Keshavarz, A., and Mehrabian, M. A., 2012, "Heat transfer enhancement of a thermal storage unit consisting of a phase change material and nano-particles," Journal of Renewable and Sustainable Energy, 4(4), p. 043124.

[35]. Esmeryan, K. D., Castano, C. E., Bressler, A. H., Abolghasemibizaki, M., and Mohammadi, R., 2016, "Rapid synthesis of inherently robust and stable superhydrophobic carbon soot coatings," Applied Surface Science, 369, pp. 341-347.
[36]. Barari, G., " "Combustion Kinetics of Advanced Biofuels" (2015). Electronic Theses and Dissertations. Paper 1444. http://stars.library.ucf.edu/etd/1444."
[37]. Barari, G., Koroglu, B., Masunov, A. E., and Vasu, S., "Combustion of Aldehydes in the Negative Temperature Coefficient Region: Products and Pathways," Proc. ASME Turbo Expo 2016, p. V003T003A012.
[38]. Barari, G., Sarathy, S. M., and Vasu, S. S., 2016, "Improved combustion kinetic model and HCCI engine simulations of di-isopropyl ketone ignition," Fuel, 164, pp. 141-150.
[39]. Barari, G. K., Batikan; Masunov, Artem; Vasu, Subith, 2016, "Products and pathways of aldehydes oxidation in the negative temperature coefficient region," Journal of Energy Resources Technology, 139(1).
[40]. Pryor, O., Barari, G., Koroglu, B., Lopez, J., Nash, L., and Vasu, S., "Shock Tube Ignition Studies of Advanced Biofuels," Proc. 52nd AIAA/SAE/ASEE Joint Propulsion Conference, p. 4691.
[41]. Makhmalbaf, M. H. M., 2012, "Experimental study on convective heat transfer coefficient around a vertical hexagonal rod bundle," Heat and Mass Transfer, 48(6), pp. 1023-1029.
[42]. Jalilian, P., Kreun, P. K., Makhmalbaf, M. M., and Liou, W. W., 2014, "Computational aerodynamics of baseball, soccer ball and volleyball," American Journal of Sports Science, 2(5), pp. 115-121.
[43]. Nicolas, R., 2007, "Fabrication de microcaloducs par écriture directe," McGill University, Montreal, p. 35.